Int. J. Electrochem. Sci., 15 **(2020)** 8041 – 8054, doi: 10.20964/2020.08.44

International Journal of
ELECTROCHEMICAL
SCIENCE
www.electrochemsci.org

N, S co-doped Graphene/Ag@Au Triangular Core-Shell Nanomaterials for Determination of Quercetin

Shaoping Feng[1,2,3], *Jiale Guo* [1,2], *Xianlan Chen*[1,2,*], *Jinming Meng*[1,2,*], *Guowei Zhang*[1,2,*], *Guiyang Liu*[1,2], *Hongyan Sun*[1,2], *Baosen Wang*[1,2], *Wei Liu*[1,2]

[1] College of Science, Honghe University, Mengzi, 661199, Yunnan, P.R.China
[2] Local Characteristic Resource Utilization and New Materials Key Laboratory of Universities in Yunnan, Honghe University, Mengzi, 661199, Yunnan, China
[3] School of Metallurgical and Ecological Engineering, University of Science and Technology Beijing, Beijing 100083, China
[*]E-mail: 13489086418@163.com, 352603936@qq.com, yunnmzh@126.com

Received: 21 March 2020 / *Accepted:* 16 May 2020 / *Published:* 10 July 2020

In the study, a hydrothermal method was used to prepare N, S co-doped graphene (NS-G) with graphenes oxide (GO) as raw material, L-cysteine ($C_3H_7NO_2S$) as sulfur source, nitrogen source and reductant. The atoms of N and S have been completely bonded to carbon atoms when the mass ratio of GO and L-cystein was 1:5. Then, the NS-G was impregnated with Ag@Au triangular core-shell nanomaterials (T-Ag@Au NPs) prepared by seed-mediated growth method to obtain N, S co-doped graphene/Ag@Au triangular core-shell nanomaterials (NS-G/T-Ag@Au NPs). The NS-G/T-Ag@Au NPs were dropped on glassy carbon electrode (GCE) to construct a novel modified electrode (NS-G/T-Ag@Au NPs/GCE) for sensing quercetin. The electrochemical sensor for quercetin determination exhibited excellent stability and sensitivity with a good linear range (0.5 μM -15.0 μM) and low the detection limits (5×10^{-8} M). The NS-G/T-Ag@Au NPs/GCE, in particular, was successfully applied for determination of quercetin in tea and honeysuckle samples with desirable recovery range (97.46-103.48 %) and relative standard deviation (RSD, 1.27-5.10 %).

Keywords: N, S co-doped graphene; T-Ag@Au NPs; Quercetin; Electrochemical sensor

1. INTRODUCTION

As a member of the flavonoid family, quercetin has been greatly founded in numerous plants, including vegetables, fruits, tea and Chinese herbal medicines [1-3]. Quercetin exhibits various biological benefits including cardiovascular protection, anticancer, anti-allergic, antiviral, lowering blood pressure and blood lipids [4, 5]. Recently, it is the quercetin that has received much attention due to its biological activities and potential pharmaceutical applications [6]. Therefore, developing a

convenient, sensitive and efficient method for analysis of quercetin in real samples is desirable and important.

Nowadays, several analytical methods for the determination of quercetin including LC-MS [7], HPLC-UV [8], HPLC-MS/MS [9], GC-MS [10], CE [11, 12] and electrochemical methods [13, 14] have been reported. However, the special properties, including the complex matrix and low content of quercetin in real samples, required high-sensitivity of the analysis methods. It is the electrochemical methods that are the most preferred due to its several advantages, such as fast, high-sensitivity and low-cost [15]. For examples, S. Selvarajan et al. constructed a novel electrochemical sensor of g-C_3N_4/NiO/GCE and employed for detection of quercetin in different real samples with a wide linear range (0.010-250 μM) and low detection limit (0.002 μM) [13]. Zhou et al. reported PB-rGO/TCD/AuNPs/GCE for determination of quercetin in juice, wine and honeysuckle and obtained a satisfactory results [16]. Zhang et al. successfully constructed MIP/MIL-101 (Cr)/MoS_2/GCE sensor and used to determinate of quercetin in honey samples with the detection limit of 0.06 μM [17]. Maryam Mosleh et al. reported MWCNTs/CPE and used for determination of quercetin in orange juice with a low detection limit (1.96 nM) [18].

In order to develop an efficient, fast and simple method with high sensitivity for determination of quercetin, N and S co-doped graphene/Ag@Au core-shell triangular nanomaterials modified electrodes (NS-G/T-Ag@Au NPs/GCE) were proposed and applied in the study. More importantly, the proposed method was sensitive and reliable for determination of quercetin in tea and honeysuckle samples with acceptable recovery and excellent stability.

2. EXPERIMENT

2.1 Reagents

$HAuCl_4$, L-cysteine ($C_3H_7NO_2S$, BR), $AgNO_3$ and ascorbic acid ($C_6H_8O_6$) were purchased from Sinopharm Chemical Reagent Co. Ltd. (Shanghai, China). Graphenes oxide (GO) was purchased from CFNANO Co. Ltd. (Nanjing, China). The phosphate buffer solution (PBS, HAc-NaAc) and ultra-pure water were used to dilute the stock solution to obtain the desired working solutions. All the other chemicals were of AR grade and used without further purification.

2.2 Instruments and characterizations

UV-vis spectra (UV 800, SHIMADZU, Japan) was used to obtain UV-vis absorption spectra of Ag seeds, triangular Ag nanomaterials (T-Ag) and T-Ag@Au NPs. XPS (Thermal Scientific K-Alpha XPS spectrometer) was employed to investigate the atomic composition of NS-G and NS-G/T-Ag@Au NPs. SEM (Nova Nano SEM 230, FEI, USA) and HRTEM (Tecnai G2 F20 S-TWIN, 200 kV, FEI Company, USA) were used to obtian the morphologies and microstructure of the materials.

The electrochemical workstation (CHI 660C, Shanghai) was used to obtain the cyclic voltammetry (CV). The electrochemical cell consisted of a three electrode system with a bare glassy

carbon electrode (GCE, 3.0 mm in diameter) or modified working electrode as a working electrode, a platinum wire as a counter electrode and Ag/AgCl electrode as a reference electrode. PBS (0.10 M, pH= 3.5) was added into the electrochemical cell and all the determination solutions were purged with N_2 for at least 15.0 min before measurements. All measurements were carried out at room temperature (25 $^{\circ}$C).

2.3 Preparation of T-Ag and T-Ag@Au NPs

Firstly, 20 mL 0.25 mM $AgNO_3$ and 20 mL 0.25 mM trisodium citrate were mixed and stirred at 25 $^{\circ}$C, and then 0.60 10 mM frozen fresh $NaBH_4$ was added and stirred for 30 s. The Ag seed was obtained when the color of the solution changed to tan. The reaction system was kept in the darkness and the seed aging time was of 12 h. After that, 0.50 mL 0.10 M ascorbic acid ($C_6H_8O_6$) was added into the solution of 10 mL 80 mM cetyl trimithyl ammonium bromide (CTAB) and shaken well. Subsequently, 0.25 mL 10 mM $AgNO_3$, 0.20 mL Ag seed solution and 0.10 mL 1.0 M NaOH were added in sequence. The mixture was stored in the darkness for 12 h to obtain T-Ag. Finally, the solution of 2000 μL Ag seeds solution and 3000 μL ultra-pure water was added into a beaker contained 13 μL 117.6 mM $HAuCl_4$ and kept for 10 min in an ice bath. Then, 1000 μL 0.1 M ascorbic acid ($C_6H_8O_6$) was added gradually into the obtained mixture and stirred for another 30.0 min in the ice bath to prepare T-Ag@Au NPs. The photographic images and UV-vis spectra of Ag seed, T-Ag and T-Ag@Au NPs were shown in Fig. 1(A) and Fig. 1(B), respectively. The SEM and TEM of T-Ag and T-Ag@Au NPs were shown in Fig. 1(C-G).

2.4 Preparation of NS-G and NS-G/T-Ag@Au NPs

In order to prepare NS-G, GO and L-cystein (mass ratio of 1:5) were mixed and heated at 180 °C for 8 h in the autoclave with magnetic agitating. The obtained mixture was centrifuged at 30000 rpm for 5.0 min, and the supernatant was removed. After that, the solution was diluted with ultra-pure water and centrifuged until the excess L-cysteine was eluted. The SEM, TEM and XPS of NG were present in Fig. 2, and Fig. 3, respectively. For NS-G/T-Ag@Au NPs preparation, T-Ag@Au NPs (350 μL), NS-G (250 μL) and ultra-pure water (400 μL) were transferred to the vortex mixer for mixing evenly until the solution with uniform dispersion was obtained. The TEM and XPS of NS-G/T-Ag@Au NPs were shown in Fig. 4.

2.5 Preparation of electrode and analytical procedure

The fabrication procedure of the modified glassy carbon electrode (GCE), including polishing, ultrasonication and drying, were as same as in our previous works [19]. Then, 7.0 μL the NS-G/T-Ag@Au NPs was uniformly dropped on the surface of the modified GCE to obtained NS-G/T-Ag@Au NPs/GCE electrode after drying with infrared lamp. Similarly, the NS-G/GCE and T-Ag@Au/GCE as

compared were fabricated. The NS-G/T-Ag@Au NPs/GCE electrode was regenerated by a multi-circle potential scan (0.0-0.8 V) in a blank PBS (pH= 3.5) until the background CV curve was invariable.

3. RESULTS AND DISCUSSION

3.1 Characterization of T-Ag and T-Ag@Au NPs

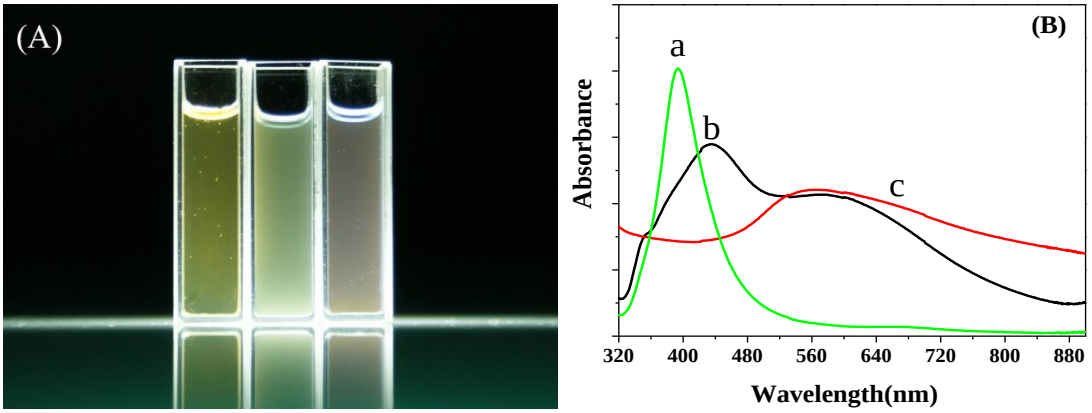

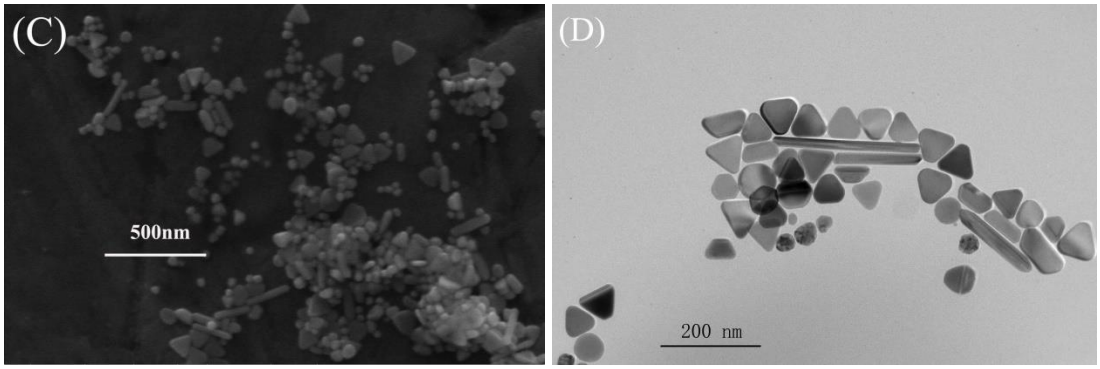

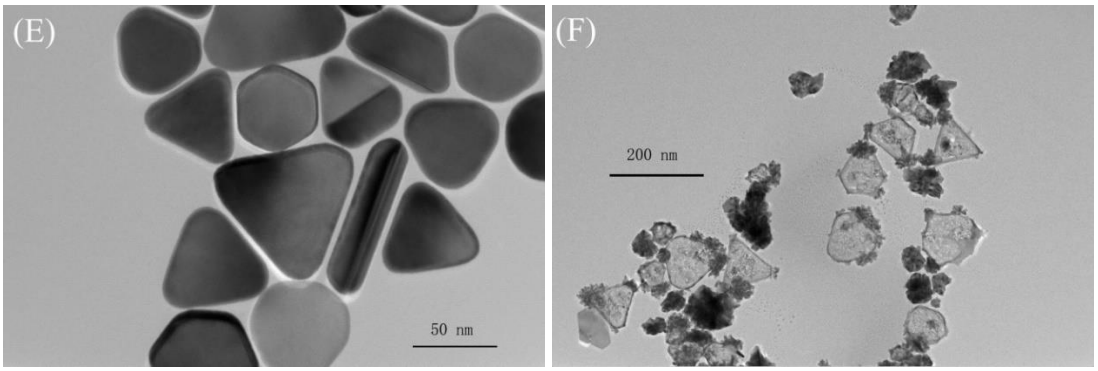

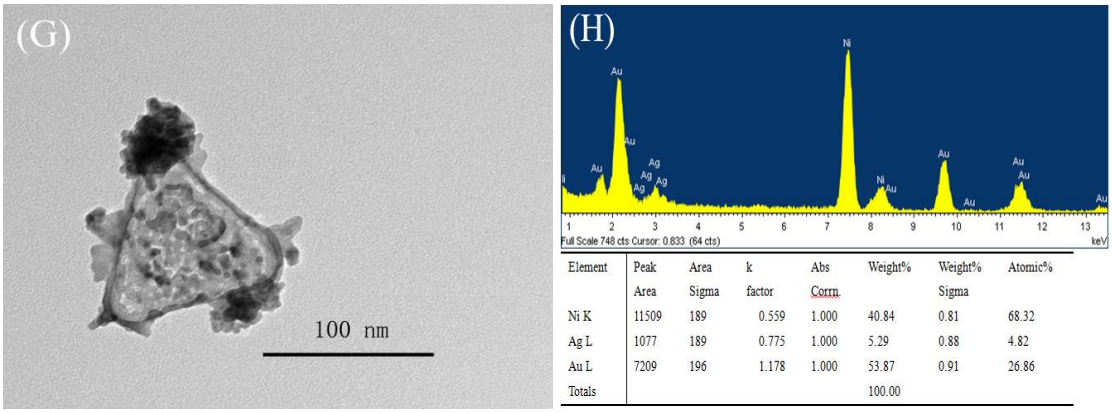

Element	Peak Area	Area Sigma	k factor	Abs Corrn	Weight%	Weight% Sigma	Atomic%
Ni K	11509	189	0.559	1.000	40.84	0.81	68.32
Ag L	1077	189	0.775	1.000	5.29	0.88	4.82
Au L	7209	196	1.178	1.000	53.87	0.91	26.86
Totals					100.00		

Figure 1. Photographic image of Ag seed, T-Ag and T-Ag@Au NPs (from left to right) (A). UV-vis spectra of (a) Ag seed, (b) T-Ag and (c) T-Ag@Au NPs (B). SEM of T-Ag (C). TEM of T-Ag at different magnification (D and E). TEM of T-Ag@Au NPs at different magnification (F and G). EDS of T-Ag@Au NPs (Ni from the nickel grid) (H).

UV-vis spectra of Ag seed, T-Ag and T-Ag@Au NPs was shown in Fig. 1(B), the absorption peak at 400 nm was referred to Ag seed (curve a) while the new absorption peaks at 445 nm and 570 nm were correspond to T-Ag (curve b) [20]. In addition, a new wide absorption peak of T-Ag@Au NPs appeared at 550 nm belonged to Au (curve c), demonstrating that Au has successfully coated on Ag core and formed T-Ag@Au NPs [21]. The SEM of T-Ag (Fig. 1(C)) showed that there were numerous T-Ag with triangular structure and little of rod-shaped and spherical nanoparticles. From Fig. 1(D) and Fig. 1(E), it can be found that the prepared T-Ag are almost triangular, uniformly distributed and neatly arranged without overlapping each other, which indicated that T-Ag has been successfully obtained. Moreover, the TEM of T-Ag@Au NPs (Fig. 1(F)) revealed that T-Ag@Au NPs were evenly distributed with hollow triangular and translucent morphology, which was attributed to the constitution of a tiny battery (Ag@Au) resulted in the dissolution of Ag. It can be seen from Fig. 1(G) that there has obvious edges of T-Ag@Au NPs with black shell (Au) and translucent core (Ag), indicating its core-shell structure. The EDS image in Fig. 1(H) showed that T-Ag@Au NPs contained an atomic ratio of 26.86% Au and 4.82% Ag. The dissolution of Ag resulted in a sharp reduction of its content, and formed a hollow translucent structure.

3.2 Characterization of N, S-doped graphene (NS-G)

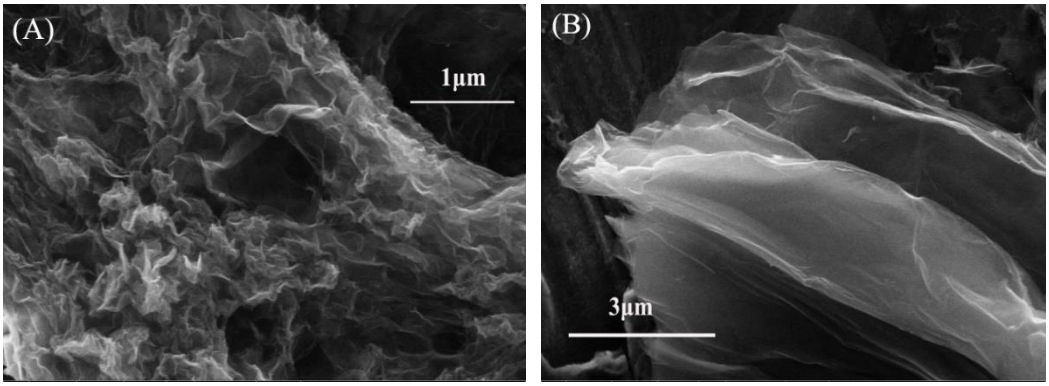

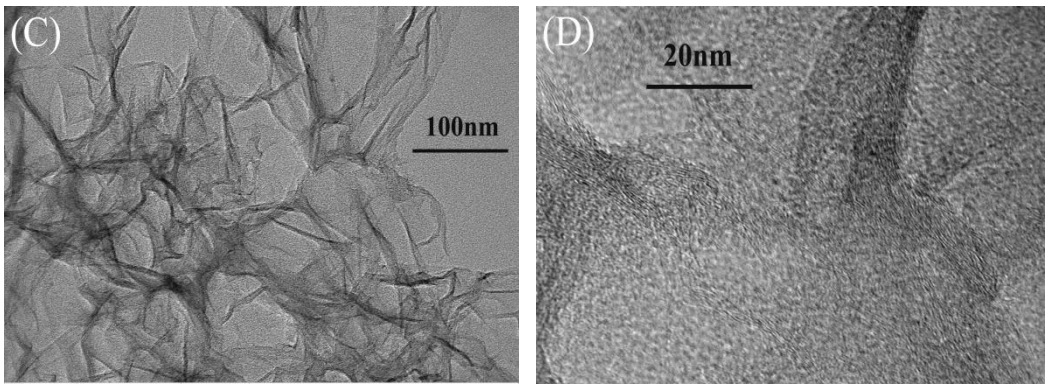

Figure 2. SEM (A and B) and TEM (C and D) of NS-G

The morphology of as-synthesized NS-G was revealed by the SEM and TEM images. As was shown in Fig. 2(A) and Fig. 2(B), a sheet-like graphene nanosheets with folded structure was obtained from the agglomerated individual layers. A transparent, disorderly and wrinkled sheet of NS-G was observed in Fig. 2(C) and Fig. 2(D), which indicated that NS-G remained the crumpled-like surface and 3D structure of the graphene.

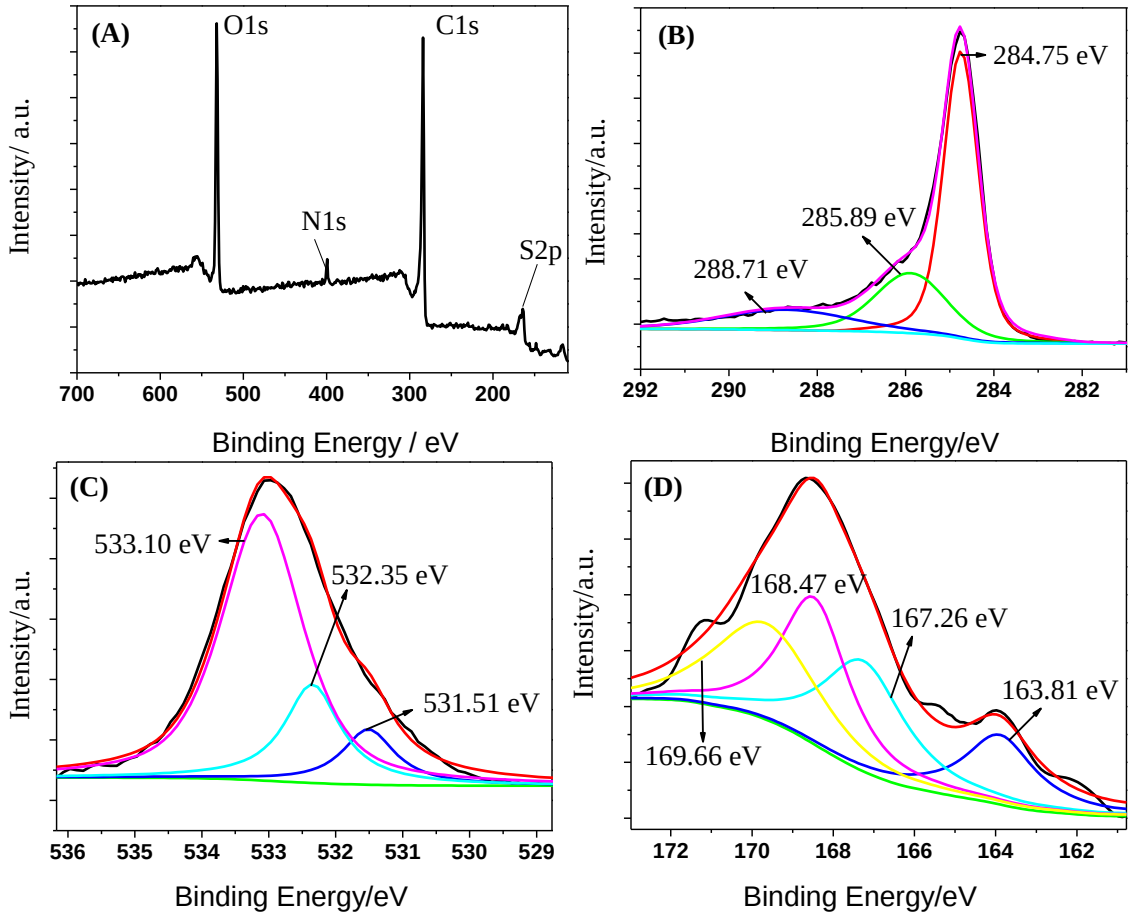

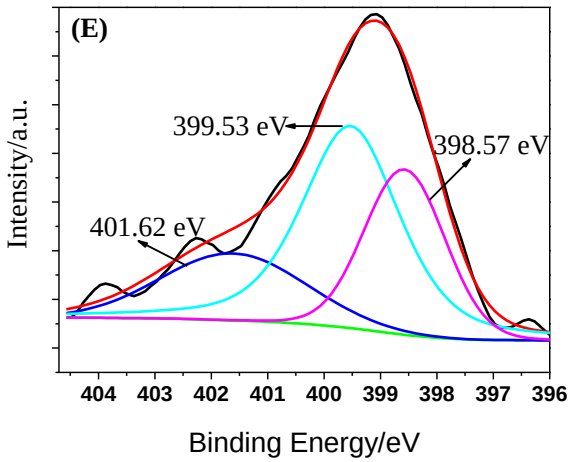

Figure 3. (A) Full-scan XPS of NS-G. (B-D) high resolution C1s, O1s, S2p and N1s XPS scan of NS-G

XPS was employed to ascertain the element components of NS-G, and the results were shown in Fig. 3. From Fig. 3(A), there were four peaks at 284.28eV (C1s), 532.03eV (O1s), 164.23eV (S2p) and 399.38eV (N1s), demonstrating that the atoms of N and S have been completely bonded to carbon atoms [22]. Three distinguishable peaks of 284.75 eV (C=C), 285.89 eV (C-C and C-N) and 288.71 eV (-COOH) were observed in Fig. 3(B) [1]. In Fig. 3(C), four fitting peaks of 531.51 eV, 532.35 eV and 533.10 eV were attributed to C=O-OH, C-O and C-OH, respectively [23]. Fig. 3(D) showed four fitting peaks of 163.81 eV (C-S-C, $2P_{3/2}$), 167.26 eV (C-S-C, $2P_{1/2}$), 168.47 eV (S-O, $2P_{3/2}$) and 169.66 eV (S-O, $2P_{1/2}$) [24]. XPS spectra of N1s was shown in Fig. 3(E), there were three peaks at 398.57 eV (pyridinic N), 399.53 eV (yrrolic N) and 401.62 eV (graphitic N) [24, 25].

3.3 Characterization of NS-G/T-Ag@Au NPs

SEM images of NS-G/T-Ag@Au NPs showed that numerous T-Ag@Au NPs were uniformly dispersed the NS-G supports, demonstrating that T-Ag@Au NPs have successfully anchored on the NS-G surface, as was shown in Fig. 4(A). XPS spectra of the Au 4f and Ag 3d in NS-G/T-Ag@Au NPs were shown in Fig. 4(B) and Fig. 4(C), respectively. The binding energies of Au $4f_{7/2}$ and Au $4f_{5/2}$ were 83.68 eV and 87.38 eV (Fig. 4(B)), respectively [26].

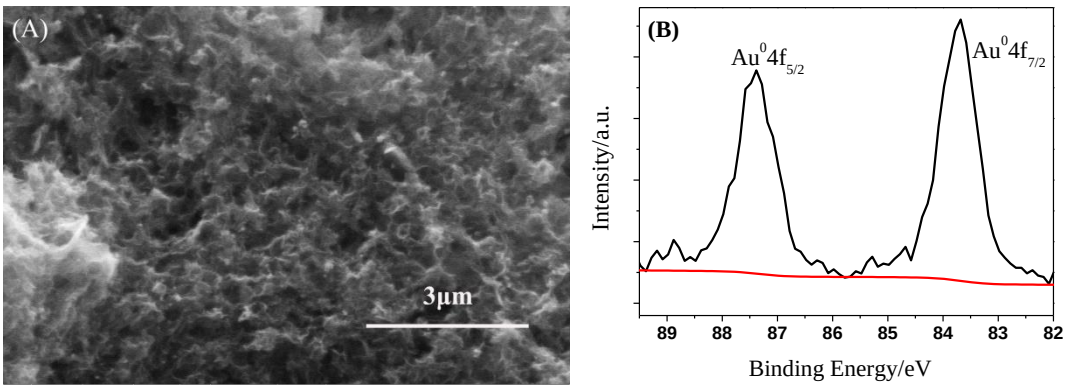

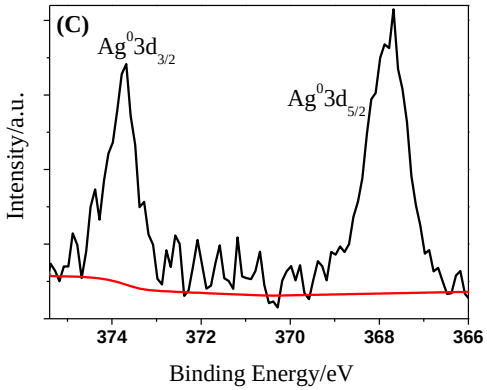

Figure 4. (A) SEM images of NS-G/T-Ag@Au NPs. (B) XPS spectra of the Au 4f in NS-G/T-Ag@Au NPs. (C) XPS spectra of the Ag 3d in NS-G/T-Ag@Au NPs.

There were two peaks at 367.68 eV ($Ag3d_{5/2}$) and 373.68 eV ($Ag3d_{3/2}$) in Fig. 4(C) [27]. Compared with the metallic Au^0 and Ag^0, a slight blue shift was obtained from Ag 3d and Au 4f, which probable reason was the electron transfer from GO sheet to T-Ag@Au NPs [28].

3.4 Electrochemical Characterization

3.4.1 Electrochemical behavior of quercetin

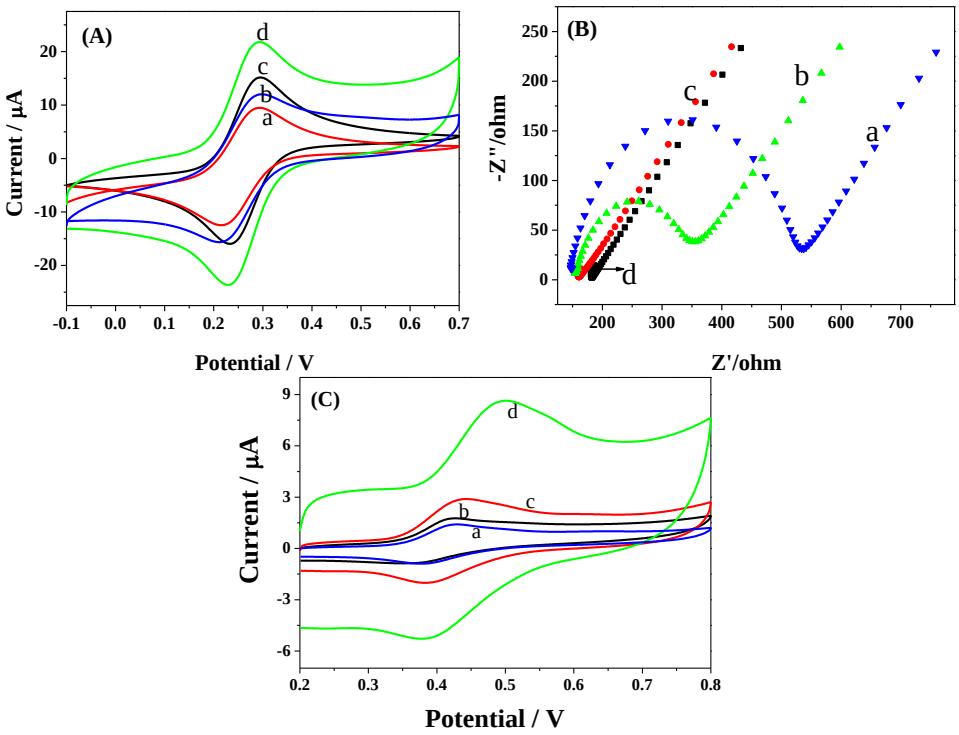

Figure 5. (A) CVs of bare GCE (a), NS-G/GCE (b), T-Ag@Au/GCE (c) and NS-G/T-Ag@Au NPs/GCE (d) in mixed solution of 0.5 M KCl and 10 mM$Fe(CN)_6^{3-}$, scan rate of 50 mV/s. (B) EIS of bare GCE (a), NS-G/GCE (b), T-Ag@Au/GCE (c) and NS-G/T-Ag@Au NPs/GCE (d) in mixed solution of 0.5 M KCl and 10 mM$Fe(CN)_6^{3-}$, 0.1 Hz~10^5 kHz. (C) CVs of bare GCE (a), NS-G/GCE (b), T-Ag@Au/GCE (c) and NS-G/T-Ag@Au NPs/GCE (d), 50 μM quercetin, pH= 3.5 (HAc-NaAc) ,scan rate of 50 mV/s.

To investigate the interface properties of modified electrodes, the voltammetric responses of bare GCE (a), NS-G/GCE (b), T-Ag@Au/GCE (c) and NS-G/T-Ag@Au NPs/GCE (d) were studied by CVs and EIS. Apparently, the NS-G/T-Ag@Au NPs/GCE (curve d) exhibits the highest peak current (I_p) in Fig 5(A), indicating that the synergistic effects of NS-G/T-Ag@Au NPs on the electrode surface and enhanced signal amplification to improve the sensitivity of immunosensor. The Nyquist plots of bare GCE (a), NS-G/GCE (b), T-Ag@Au/GCE (c) and NS-G/T-Ag@Au NPs/GCE (d) were shown in Fig. 5B. It is the NS-G/T-Ag@Au NPs/GCE (curve d) that owned the smallest value of electron transfer resistance (R_{et}), implying the excellent electro-conductibility of NS-G/T-Ag@Au NPs, which resulted from the tuning of electronic structure after N and S co-doping. CVs of 50 μM quercetin on different electrodes were tested and recorded in Fig. 5(C). A relatively poor redox peaks on the bare GCE (curve a), NS-G/GCE (curve b) and T-Ag@Au/GCE (curve c), which indicated the little active sites for electrochemical reaction and weak adsorption of quercetin. However, a well-defined redox peaks were observed on NS-G/T-Ag@Au NPs/GCE (curve d), demonstrating the improved catalytic effect to quercetin. Therefore, NS-G/T-Ag@Au NPs/GCE can sensitively determinate of quercetin.

3.4.2 Effect of the accumulation time and accumulation potential

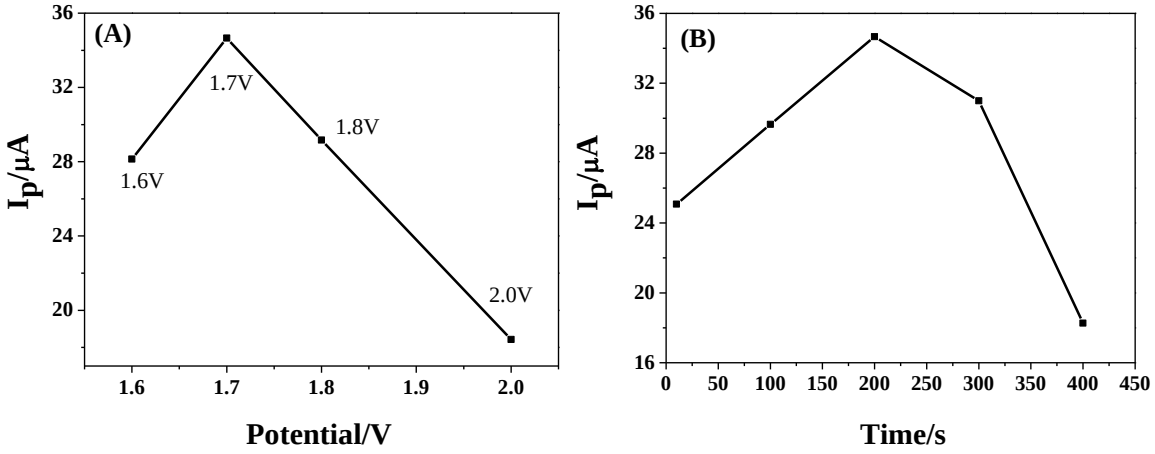

Figure 6. (A) The effect of accumulation potential on I_p. (B) The effect of accumulation time on I_p. 50 μM quercetin, pH = 3.5 (HAc-NaAc)

The effect of accumulation potential and accumulation time on the determination of 50 μM quercetin in PBS (pH = 3.5) has been investigated. The I_p reached to the maximum when accumulation potential was 1.7 V (Fig. 6(A)), which demonstrated that the best accumulation potential was 1.7 V for detection of quercetin and used in further experiments. Usually, the accumulation time was a significant paremeter to determination of analyzes in the electrochemical analysis method. In Fig. 6(B), the I_p of quercetin increased steeply with the increasing of accumulation time before 200 s, and then decreased obviously as the accumulation time increased from 200 to 400 s. Thus, 200 s of accumulation time was a suitable optimum for quercetin analysis in this study.

3.4.3 Influence of pH

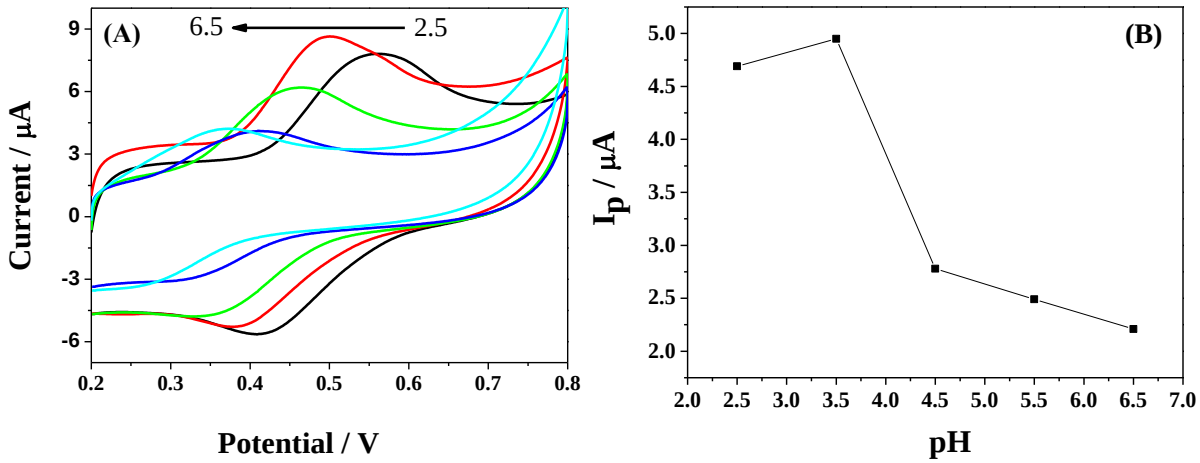

Figure 7. (A) CVs of NS-G/T-Ag@Au NPs/GCE in PBS with different pH values (2.5, 3.5, 4.5, 5.5, 6.5). (B) The effect of pH on I_p. 50 μM quercetin, scan rate of 50 mV/s.

The electrochemical responses of 50 μM quercetin on NS-G/T-Ag@Au NPs/GCE with different pH values (2.5, 3.5, 4.5, 5.5, 6.5) at 50 mV/s were investigated and shown in Fig. 7(A). The maximum value of I_p was obtained when pH value reached to 3.5, and then decreased steeply with the increasing of pH value (Fig. 7(B)). Thus, pH 3.5 was selected as the suitable pH for sensitively determination of quercetin.

3.4.4 Effect of scan rate

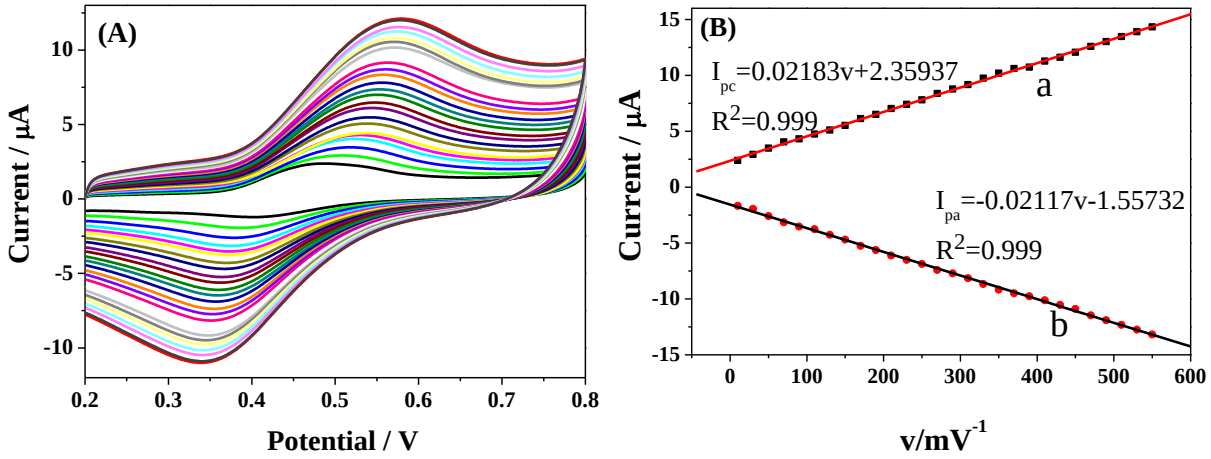

Figure 8. (A) CVs of NS-G/T-Ag@Au NPs/GCE. 50 μM quercetin, pH= 3.5(HAc-NaAc), scan rate: 10-550 mV/s). (B) Linear relationship of I_p versus vs. scan rate.

The CVs of NS-G/T-Ag@Au NPs/GCE in 10 mL PBS (pH= 3.5) containing 50 μM quercetin at different scan rates (10-550 mV/s) were recorded (Fig. 8). The I_p increased gradually and the peaks distance exhibited an obvious enlargement when the scan rate increased from 10 to 550 mV/s (Fig. 8(A)). Moreover, the surface-controlled process has been ascertained due to the good linear

relationship between I_p (the anode peak currents (I_{pa}) and the cathode peak currents (I_{pc})) and the scan rate from 10 to 550 mV/s (Fig. 8(B)) [29].

3.4.5 Determination of quercetin on NS-G/T-Ag@Au NPs/GCE

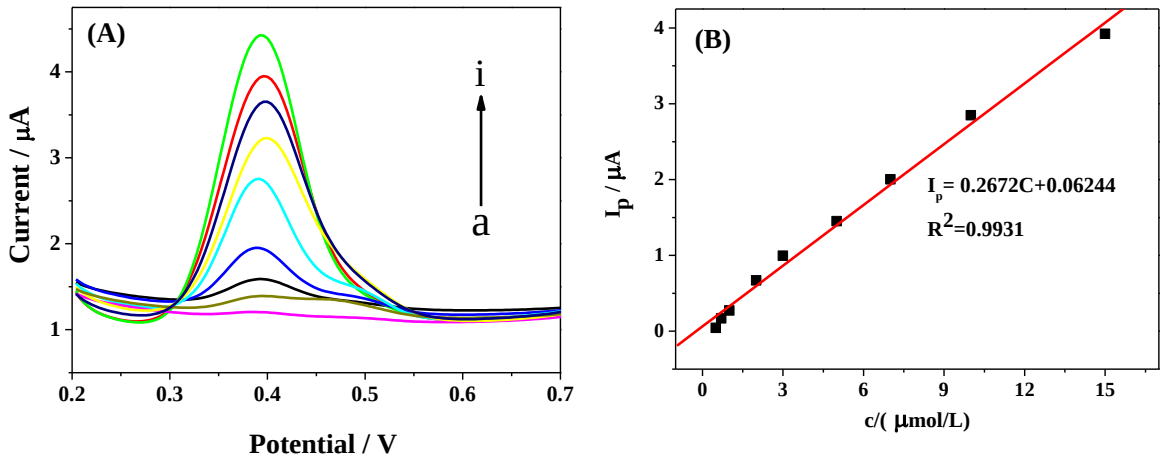

Figure 9. (A) DPV on NS-G/T-Ag@Au NPs/GCE, pH=3.5 (HAc-NaAc solution).Quercetin concentrations: 0.5 μM, 0.7 μM, 1.0 μM, 2.0 μM, 3.0 μM, 5.0 μM, 7.0 μM, 10.0 μM, 15.0 μM. (B) The relationship of I_p with quercetin concentrations.

The DPV was employed for the determination of quercetin in this study and the the results were present in Fig. 9(A). The I_p was linear to the quercetin concentration at NS-G/T-Ag@Au NPs/GCE in the range of 0.5 μM-15.0 μM. From Fig. 9(B), the regression equation was: I_p= 0.2672C (μM) + 0.06244 with the R^2= 0.9931, and the detection limits was 5×10^{-8} M (S/N=3), implying that quercetin can be accurately determined using NS-G/T-Ag@Au NPs/GCE. The comparison of similar electrodes and NS-G/T-Ag@Au NPs/GCE for quercetin determination was shown in Table 1.

Table 1. Comparison of similar electrodes and NS-G/T-Ag@Au NPs/GCE for quercetin determination

Electrodes	Linear range	Detection limit	Samples	Reference
CTAB-cMWCNTs/MWCPE	0.01-1.0 μM 2.0-20.0 μM.	5.3 nM	*Rhizoma kaempferiae*	[4]
g-C_3N_4/NiO/GCE	0.010-250 μM	0.002 μM	Tea, apple and honeysuckle	[13]
PB-rGO/TCD/Au NPs/GCE	0.005-0.4 μM	1.83 nM	Apple juice, red wine and honeysuckle	[16]
MIP/MIL-101 (Cr)/MoS_2/GCE	0.1-700 μM,	0.06 μM	Honey samples	[17]
MWCNTs/CPE	< 1.0 μM	1.96 nM	Orange juice	[18]
NS-G/T-Ag@Au NPs/GCE	0.5-15.0 μM	5×10^{-8} M	Tea and honeysuckle	This work

3.4.6 Stability of the NS-G/T-Ag@Au NPs/GCE

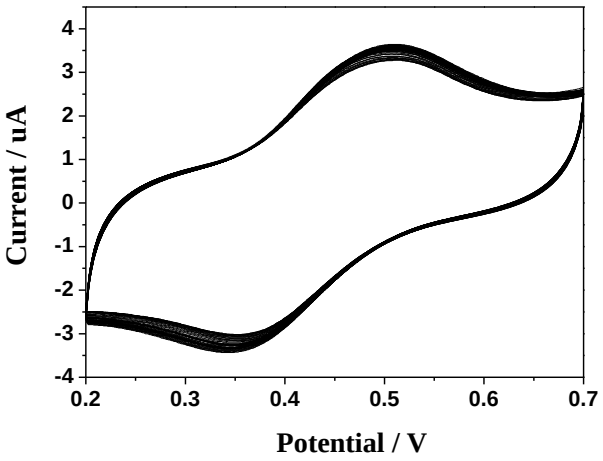

Figure 10. CVs of quercetin electrocatalytic reaction at NS-G/T-Ag@Au NPs/GCE in 10 mL PBS (pH = 3.5) containing 25 μM quercetin for 55 consecutive cycles.

The NS-G/T-Ag@Au NPs/GCE was used to determination of quercetin and scanned continuously for 55 cycles at a scan rate of 50 mV/s in order to estimate its stability. Obviously, the CVs curves of quercetin electrocatalytic reaction at NS-G/T-Ag@Au NPs/GCE change litter after 55 consecutive cycles (Fig. 10), indicating an excellent stability of NS-G/T-Ag@Au NPs.

3.4.7 Sample analysis

Table 2. Results of quercetin determination in Pu'er tea and Honeysuckle samples (n=3).

Sample	Original (μM)	Added (μM)	Found (μM)	Recovery (%)	RSD (%)
Pu'er tea	0.8269	5.00	5.70	97.46	2.06
		10.00	11.00	101.73	3.65
		15.00	15.80	99.82	1.27
Honeysuckle	7.41×10^{-2}	5.00	5.08	100.12	5.10
		10.00	10.07	99.96	4.50
		15.00	15.50	103.48	4.90

In order to estimate the feasibility and applicability of the NS-G/T-Ag@Au NPs/GCE, the quercetin concentration of real samples (Pu'er tea and honeysuckle). 0.50g of Pu'er tea and honeysuckle samples were accurately weighed and added in 50 mL boiled water with heating for 10 min. An accurate volume of the solution was diluted to 100 mL with PBS (pH= 3.5) to obtain the desired working solution for quercetin determination after filtering. The DPV results showed that the recovery was 97.46-103.48 % and the RSD were 1.27-5.10 % (Table 2), demonstrating that the proposed method was reasonable for quercetin determination in tea and honeysuckle samples.

4. CONCLUSIONS

In brief, N, S co-doped graphene (NS-G) has been synthesized by a hydrothermal method with graphenes oxide (GO) as raw material, L-cysteine ($C_3H_7NO_2S$) as sulfur source, nitrogen source and reductant. Then, Ag@Au triangular core-shell nanomaterials (T-Ag@Au NPs) were successfully embedded in NS-G to obtain N, S co-doped graphene/Ag@Au triangular core-shell nanomaterials (NS-G/T-Ag@Au NPs). Specially, a novel modified electrode of NS-G/T-Ag@Au NPs/GCE was constructed and exhibited an excellent response with a good linear range (0.5-15.0 μM) and low the detection limits (5×10^{-8} M) for quercetin determination. The as-prepared NS-G/T-Ag@Au NPs/GCE was successfully applied for determination of quercetin in tea and honeysuckle samples with high accuracy and excellent stability.

ACKNOWLEDGMENTS

The authors gratefully acknowledge the financial support from the Yunnan education department of Scientific Research Foundation (2018JS478, 2019J1183), Yunnan Local Colleges Applied Basic Research Projects (2018FH001-114, 2018FH001-049 and 2017FD157) and the National Natural Science Foundation of China (51362012, 51662007 and 51574213).

References

1. F.Y. Kong, L. Yao, R.F. Li, H.Y. Li, Z.X. Wang, W.X. Lv, W. Wang, *J. Alloys Compd.*, 797 (2019) 413-420.
2. H. Wu, M. Chen, Y. Fan, F. Elsebaei, Y. Zhu, *Talanta*, 88 (2012) 222-229.
3. A.T.E. Vilian, P. Puthiaraj, C.H. Kwak, S.R. Choe, Y.S. Huh, W.S. Ahn, Y.K. Han, *Electrochim. Acta*, 216 (2016) 181-187.
4. Z. Liang, H. Zhai, Z. Chen, S. Wang, H. Wang, S. Wang, *Sens. Actuators, B*, 244 (2017) 897-906.
5. D. Xiao, D. Yuan, H. He, M. Gao, *J. Lumin.*, 140 (2013) 120-125.
6. V. Pilařová, K. Plachká, L. Chrenková, I. Najmanová, P. Mladěnka, F. Švec, O. Novák, L. Nováková, *Talanta*, 185 (2018) 71-79.
7. Y. Yao, X. Ma, T. Li, H. Guo, R. Chang, J. Liu, Q. Liu, H. Hao, T. Huang, W. Chen, J. Wen, T. Zhou, *J. Pharm. Biomed. Anal.*, 161 (2018) 444-454.
8. E. Ranjbari, P. Biparva, M.R. Hadjmohammadi, *Talanta*, 89 (2012) 117-123.
9. N. Boke Sarikahya, A.C. Goren, S. Kirmizigul, *J. Pharm. Biomed. Anal.*, 173 (2019) 120-125.
10. C. Wang, Y. Zuo, *Food Chem.*, 128 (2011) 562-568.
11. S.P. Wang, K.J. Huang, *J. Chromatogr. A*, 1032 (2004) 273-279.
12. W. Wang, P. Lin, L. Ma, K. Xu, X. Lin, *J. Sep. Sci.*, 39 (2016) 1357-1362.
13. S. Selvarajan, A. Suganthi, M. Rajarajan, *Ultrason. Sonochem.*, 41 (2018) 651-660.
14. Y. Zou, F. Yan, T. Zheng, D. Shi, F. Sun, N. Yang, L. Chen, *Talanta*, 135 (2015) 145-148.
15. J.B. Raoof, R. Ojani, M. Amiri-Aref, M. Baghayeri, *Sens. Actuators, B*, 166-167 (2012) 508-518.
16. Z. Zhou, C. Gu, C. Chen, P. Zhao, Y. Xie, J. Fei, *Sens. Actuators, B*, 288 (2019) 88-95.
17. W. Zhang, L. Zong, G. Geng, Y. Li, Y. Zhang, *Sens. Actuators, B*, 257 (2018) 1099-1109.
18. M. Mosleh, S.M. Ghoreishi, S. Masoum, A. Khoobi, *Sens. Actuators, B*, 272 (2018) 605-611.
19. X. Chen, G. Yang, S. Feng, L. Shi, Z. Huang, H. Pan, W. Liu, *Appl. Surf. Sci.*, 402 (2017) 232-244.
20. M. Tsuji, S. Hikino, M. Matsunaga, Y. Sano, T. Hashizume, H. Kawazumi, *Mater. Lett.*, 64 (2010) 1793-1797.
21. Y. Chen, W.G. Wang, S. Zhou, *Mater. Lett.*, 65 (2011) 2649-2651.

22. S. Gao, H. Liu, K. Geng, X. Wei, *Nano Energy,* 12 (2015) 785-793.
23. S. Wang, S. Liu, J. Zhang, Y. Cao, *Talanta,* 198 (2019) 501-509.
24. W. Xiong, H. Li, R. Cao, *Inorg. Chem. Commun.*, 114 (2020) 107848.
25. S.A. Wohlgemuth, R.J. White, M.G. Willinger, M.M. Titirici, M. Antonietti, *Green Chem.*, 14 (2012) 1515.
26. H.G. Boyen, G. Kastle, F. Weigl, B. Koslowski, C. Dietrich, P. Ziemann, J.P. Spatz, S. Riethmuller, C. Hartmann, M. Moller, G. Schmid, M.G. Garnier, P. Oelhafen, *Sci.*, 297 (2002) 1533-1536.
27. S.T. Rajan, A.K. Nanda Kumar, B. Subramanian, *CrystEngComm*, 16 (2014) 2835-2844.
28. H. K, R.P. Joshi, S. D.V, V.N. Bhoraskar, S.D. Dhole, *Appl. Surf. Sci.*, 389 (2016) 1050-1055.
29. R. Abdel-Hamid, E.F. Newair, *J. Electroanal. Chem.*, 704 (2013) 32-37.